Studies on Deacetoxycephalosporin C Synthase Support a Consensus Mechanism for 2-Oxoglutarate Dependent Oxygenases

ARTICLE *in* BIOCHEMISTRY · MARCH 2014

Impact Factor: 3.02 · DOI: 10.1021/bi500086p · Source: PubMed

10 AUTHORS, INCLUDING:

Ivanhoe K H Leung
University of Auckland
22 PUBLICATIONS **476** CITATIONS
SEE PROFILE

Luc Henry
École Polytechnique Fédérale de Lausanne
8 PUBLICATIONS **80** CITATIONS
SEE PROFILE

Aman Iqbal
University of Toronto
6 PUBLICATIONS **28** CITATIONS
SEE PROFILE

Timothy D W Claridge
University of Oxford
217 PUBLICATIONS **4,916** CITATIONS
SEE PROFILE

BIOCHEMISTRY
including biophysical chemistry & molecular biology

Article

pubs.acs.org/biochemistry

Studies on Deacetoxycephalosporin C Synthase Support a Consensus Mechanism for 2-Oxoglutarate Dependent Oxygenases

Hanna Tarhonskaya,[#] Andrea Szöllössi,[#] Ivanhoe K. H. Leung, Jacob T. Bush, Luc Henry,[†] Rasheduzzaman Chowdhury, Aman Iqbal,[‡] Timothy D. W. Claridge, Christopher J. Schofield,* and Emily Flashman*

Chemistry Research Laboratory, University of Oxford, 12 Mansfield Road, Oxford, OX1 3TA, United Kingdom

Supporting Information

ABSTRACT: Deacetoxycephalosporin C synthase (DAOCS) catalyzes the oxidative ring expansion of penicillin N (penN) to give deacetoxycephalosporin C (DAOC), which is the committed step in the biosynthesis of the clinically important cephalosporin antibiotics. DAOCS belongs to the family of non-heme iron(II) and 2-oxoglutarate (2OG) dependent oxygenases, which have substantially conserved active sites and are proposed to employ a consensus mechanism proceeding via formation of an enzyme·Fe(II)·2OG·substrate ternary complex. Previously reported kinetic and crystallographic studies led to the proposal of an unusual "ping-pong" mechanism for DAOCS, which was significantly different from other members of the 2OG oxygenase superfamily. Here we report pre-steady-state kinetics and binding studies employing mass spectrometry and NMR on the DAOCS-catalyzed penN ring expansion that demonstrate the viability of ternary complex formation in DAOCS catalysis, arguing for the generality of the proposed consensus mechanism for 2OG oxygenases.

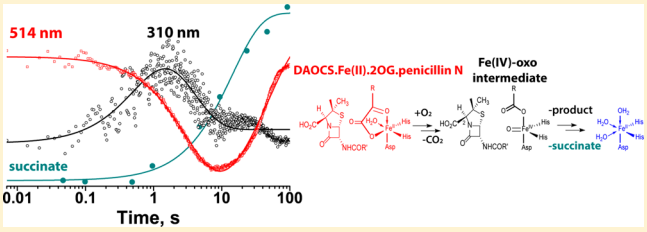

Non-heme iron(II) and 2-oxoglutarate (2OG) dependent oxygenases are a very widely distributed superfamily of enzymes, which catalyze a range of two-electron substrate oxidations.[1] Oxidation of their "prime" substrate is coupled with the oxidative decarboxylation of 2OG to give succinate and carbon dioxide. In animals, 2OG oxygenases catalyze hydroxylations and demethylations (via hydroxylation); however, in plants and microorganisms they catalyze a much wider range of oxidative reactions including desaturation, oxidative ring closure, rearrangement, and halogenation.[2−5] Extensive crystallographic analyses on 2OG oxygenases and related enzymes have revealed a common double-stranded β-helix core fold that supports a highly (but not universally) conserved "triad" of Fe(II) binding residues (reviewed in refs 3−6), typically comprising an HXD/E···H triad of residues. The 2-oxoacid of 2OG binds to Fe(II) in a bidentate manner via its ketone and C-1 carboxylate groups. The C-5 carboxylate of 2OG is normally bound by several residues including one with a basic (lysine or arginine) side chain.[3,4]

Combined kinetic, spectroscopic, and crystallographic studies have led to the proposal of a consensus mechanism for 2OG dependent oxygenases.[1,3,4,7−11] In this mechanism, 2OG binding to the active site takes place after that of ferrous iron and leads to the displacement of two water molecules (Figure 1). Subsequent binding of the "prime" substrate weakens coordination of another metal-bound water molecule, vacating a binding site for dioxygen.[12,13] The precise mechanism of dioxygen activation is not determined but likely includes dioxygen binding to the iron(II), followed by an electron transfer. Subsequent oxidative decarboxylation of 2OG then occurs to give carbon dioxide, succinate, and a ferryl intermediate (which has been observed spectroscopically).[3,14−17] The ferryl group enables "prime" substrate oxidation, at least in some cases including ring expansion, probably via a radical process.[18−20] Inhibition by the succinate product and by high concentrations of 2OG have been observed in some cases.[21] Turnover of 2OG in the absence of the "prime" substrate is also commonly observed (uncoupled turnover), however, at a lower rate than in the presence of a substrate. Overall, there is considerable evidence for this consensus mechanism from crystallographic and spectroscopic studies on multiple enzymes.[3,7,8,10,12]

Deacetoxycephalosporin C synthase (DAOCS), which is a 2OG oxygenase found in some prokaryotes, including *Streptomyces clavuligerus*, catalyzes the oxidative ring expansion of penicillin N (penN) to deacetoxycephalosporin C (DAOC).[22−26] This is the committed step in the biosynthesis of the medicinally important cephalosporin antibiotics.[22−24,27,28] Deacetoxycephalosporin/deacetylcephalosporin C synthase (DAOC/DACS) is a closely related bifunctional enzyme, which in a separate catalytic cycle catalyzes C-3′ hydroxylation of the deacetoxycephalosporin C product.[22] DAOCS also catalyzes low levels of the C-3′ hydroxylation reaction, but in organisms that contain the (almost)

Received: January 21, 2014
Revised: March 28, 2014
Published: March 31, 2014

dx.doi.org/10.1021/bi500086p | *Biochemistry* 2014, 53, 2483−2493

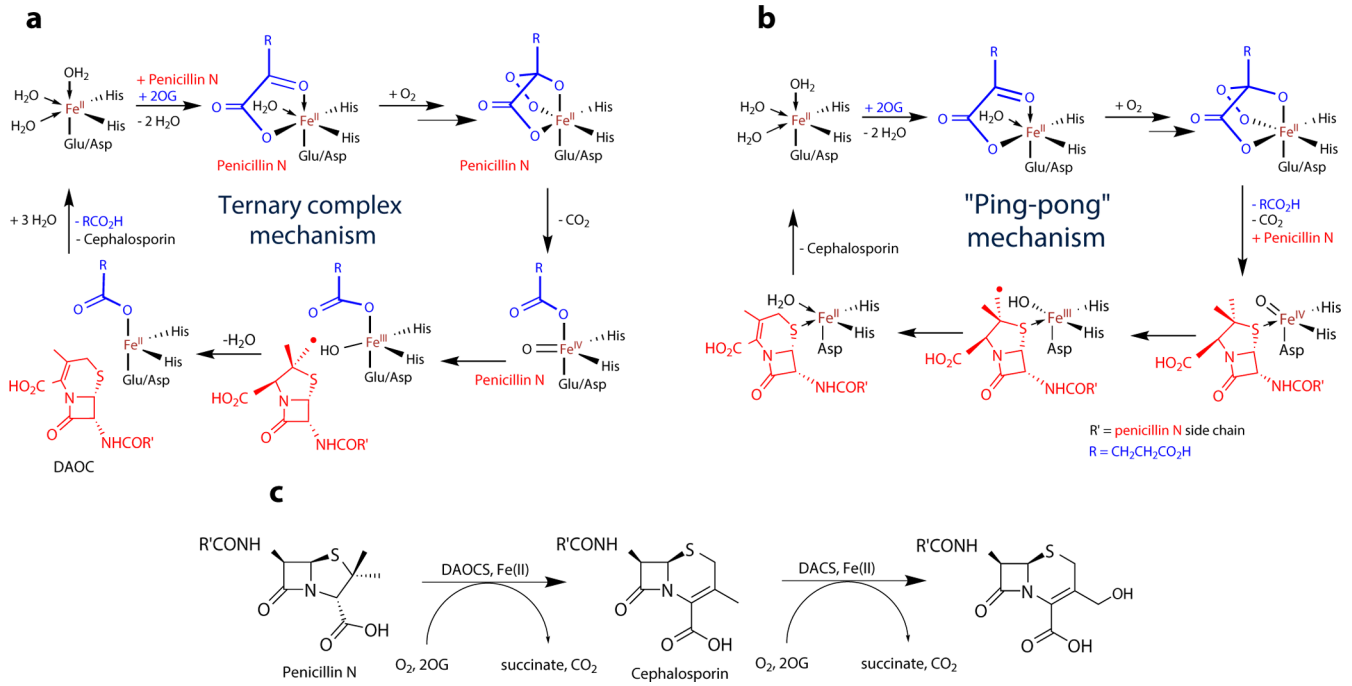

Figure 1. Mechanistic possibilities for DAOCS: (a) Outline of the proposed consensus mechanism of 2OG oxygenases, as applied to deacetoxycephalosporin C (DAOC), compared with (b) the alternative proposed mechanism.[32] (a) Binding of dioxygen to DAOCS·Fe(II)·2OG·penicillin N (penN) complex results in the oxidative decarboxylation of 2OG and generation of an Fe(IV)-oxo species that enables oxidative rearrangement of the substrate via initial hydrogen abstraction on the methyl group of the penicillin. (b) Binding of dioxygen to DAOCS·Fe(II)·2OG complex occurs with subsequent formation of an Fe(IV)-oxo species and release of succinate and CO_2 followed by penicillin binding. (c) Scheme of the DAOCS-catalyzed oxidative ring expansion of penN to DAOC and the subsequent DACS-catalyzed hydroxylation of DAOC.

"monofunctional" DAOCS, another "monofunctional" enzyme, deacetylcephalosporin C synthase (DACS), is responsible for the hydroxylation reaction, which has low levels of DAOCS ring expansion activity.[23,24] A crystal structure of DAOCS was the first reported for a 2OG oxygenase and is closely related to that of the isopenicillin N synthase, which catalyzes the four-electron bicyclization of a peptide to give the penicillin nucleus.[29,30] Structures for DAOCS in complex with Fe(II) and 2OG have also been reported, and they are consistent with those analogous complexes for other 2OG oxygenases, at least in terms of coordination chemistry and 2OG side chain binding.[3,4,29]

The oxidative ring expansion reaction catalyzed by DAOCS is unique in enzymology but is related to the synthetic "Morin rearrangement" in which a penicillin-sulfoxide undergoes rearrangement/ring expansion to give a cephem.[31] In the DAOCS-catalyzed reaction, it is proposed that a ferryl intermediate performs hydrogen abstraction from the (*pro-S*) β-methyl group of the penicillin to give a methylene radical,[19,20] which subsequently undergoes ring expansion to give a cepham radical. The radical can then react with the Fe(III)-OH species to give a cephem (DAOC) and water.[18−20,22,23]

Crystallographic analyses of DAOCS with penicillin G (penG), which serves as an analogue for the natural substrate, penN, led to the proposal that penicillin substrate binding must require displacement of 2OG or the subsequently formed succinate, because of the apparently overlapping binding sites of a "prime" substrate and cosubstrate.[32] Primarily on the basis of these crystallographic analyses (Figure S10, Supporting Information), quantum mechanical calculations and limited steady-state kinetic data, an unprecedented mechanism was proposed for DAOCS;[32] in this mechanism 2OG first undergoes conversion to succinate and carbon dioxide (without binding of penicillin to the active site) to give an iron-oxo intermediate (Figure 1b). Subsequent release of succinate from the active site enables binding of the penicillin, which can then react with the iron-oxo intermediate and undergo oxidative rearrangement (Figure 1b). The oxidative ring expansion likely occurs via a radical mechanism involving the β-methyl group of the penicillin nucleus as in the ternary complex mechanism.[20,32,33] This proposed novel "ping-pong" mechanism is unprecedented in the enzymatic family of 2OG oxygenases.

Here we report detailed kinetic and binding studies on the DAOCS-catalyzed reaction. The results provide strong evidence for the catalytic viability of the formation of the ternary DAOCS·Fe(II)·2OG·penN complex and hence imply that a consensus mechanism similar to other 2OG oxygenases can operate in DAOCS catalysis.

MATERIALS AND METHODS

Enzyme Purification. Recombinant DAOCS was produced in *Escherichia coli* BL21(DE3) and purified as reported;[34] DAOCS was incubated with EDTA to remove metals from the active site and then buffer exchanged in the suitable buffer. The recombinant DAOCS was assessed by SDS-PAGE and LC−MS and was >95% pure.

Nondenaturing Mass-Spectrometry Experiments. The DAOCS solution was buffer exchanged into 15 mM ammonium acetate pH 7.5 buffer. Samples containing 15 μM enzyme, cofactors, and substrates were prepared using concentrated stock solutions.[35] Data were acquired on a Q-TOF mass spectrometer (Q-TOF micro, Waters, Altrincham, UK) linked to a Nanomate (Advion Biosciences, Ithaca, NY, USA) with a chip voltage of 1.80 kV and a delivery pressure

dx.doi.org/10.1021/bi500086p | *Biochemistry* 2014, 53, 2483−2493

0.50 psi (1 psi = 6.81 kPa). The sample cone voltage was typically 60 or 80 V with a source temperature of 40 °C and an acquisition/scan time of 10 s/1 s. The pressure at the interface between the atmospheric source and the high vacuum region was fixed at 6.60 mbar. Data were processed with MASSLYNX 4.0 (Waters).

NMR Experiments. For enzymatic turnover experiments, unless otherwise stated, the concentrations of DAOCS, $(NH_4)_2Fe(SO_4)_2$, and L-ascorbate were maintained at 5 μM, 50 μM, and 0.1 mM respectively. Reaction mixtures were buffered using 50 mM Tris-d_{11} (pH 7.5) in 90% H_2O and 10% D_2O The reaction was carried out at 298 K in a 5 mm diameter NMR tube and initiated by the addition of DAOCS. ^{1}H NMR spectra were recorded using a Bruker AVII 500 spectrometer equipped with a 5 mm inverse TXI probe. Spectra were obtained at 93 s interval (typically 8 transient per spectrum with a relaxation delay of 1−2 s). Water suppression was achieved by the excitation sculpting method (2 ms Sinc1.1000 pulse).

For water relaxation experiments,[36,37] apo-DAOCS (200 μM) was used. Solutions were buffered using 50 mM Tris-d_{11} (pH 7.5) in 12.5% H_2O and 87.5% D_2O and 125 mM NaCl. The final concentration of Mn(II) was 50 μM (final volume 160 μL). Experiments were recorded using a Bruker AVII 500 instrument equipped with a 5 mm inverse TXI probe, and 3 mm MATCH tubes were used throughout. Saturation recovery ($90°_x$−G_1−$90°_y$−G_2−$90°_x$−G3−τ−acq) experiments were performed with 1−2 scans with a relaxation delay of at least 5 times T_1 between transients. The gradient pulses were achieved using 1 ms Sinebell gradient pulse (G_1 = 40%; G_2 = 27.1%; G_3 = 15%). The receiver gain was set to minimum value (rg = 1) to prevent receiver overload. Typically, 10−16 delay points varied between 100 ms and 60 s were used. T_1 values were obtained using the Bruker T_1/T_2 relaxation option and peak area was used for curve fitting. The titrant (typically ∼1 μL) was added using a 5 μL plunger-in-needle syringe (SGE), and sample mixing was conducted using a 250 μL gastight syringe (SGE). Binding constants were obtained by nonlinear curve fitting using OriginPro 8.0 (OriginLab) with the equation described by Morton et al.[38]

For displacement experiments,[39] ^{1}H-^{13}C 1D-HSQC experiments were conducted at 700 MHz using a Bruker Avance III spectrometer equipped with an inverse TCI cryoprobe optimized for ^{1}H observation. The CLIP-HSQC sequence was used (without ^{13}C decoupling). Typical experimental parameters were as follows: acquisition time 0.58 s, relaxation delay 2 s, number of transients 256−1600. The $^1J_{CH}$ was set to 145 or 160 Hz. For the selective version of the experiment, a 6.8 ms Q3 180 degree pulse was used, and selective irradiation was applied at the appropriate [^{13}C] chemical shift. For the nonselective version, an adiabatic 180 deg 0.5 ms CHIRP (Crp80, 0.5, 20.1) pulse was used. Three millimeter MATCH tubes with a 160 μL final sample volume were used. Solutions were buffered using Tris-d_{11} 50 mM (pH 7.5) dissolved in 95% H_2O/5% D_2O. Assays were conducted at 298 K in solutions typically containing 50 μM apo-DAOCS, 400 μM Zn(II), 50 μM 1,2,3,4-[^{13}C]-2OG or [^{13}C]-labeled NOG (^{13}C label at CH_2) or [^{13}C]-labeled penG (^{13}C label at CH_2) and excess penG or bicyclic inhibitor (IOX3). Selective irradiation was applied at 30.5 ppm for [^{13}C]-2OG and 41.8 ppm for [^{13}C]-labeled penG.

UV−vis Experiments. UV−vis spectroscopy experiments were performed as described.[14] An anaerobically prepared assay mixture contained 200 μM DAOCS in Hepes 50 mM pH 7.5 with 200 μM Fe(II), 2.5 mM 2OG, and 2 mM substrate. Data were presented as difference spectra after subtraction of the DAOCS spectrum to reveal metal ligand charge transfer (MLCT) features.

Stopped-Flow Kinetics. Stopped-flow UV−vis spectroscopy experiments were performed as described.[14] An anaerobically prepared assay mixture containing 0.8 mM DAOCS, 1 mM substrate, 5 mM 2OG, 0.7 mM Fe(II) was rapidly mixed with O_2-free/O_2-saturated buffer at 5 °C. The reaction was observed over 1000 s using a photodiode array detector, and the difference spectra were analyzed (a spectrum of the reaction with O_2-free buffer was subtracted from the one with O_2-saturated buffer). Kinetic traces representing identified absorbance features were fitted with a double exponential function using OriginPro 8.0 (OriginLab) software and analyzed.

Rapid Quench Flow Kinetics. Rapid quench flow experiments were performed using the same conditions and procedure of preparation of the assay mixture as in stopped-flow experiments. TG-K scientific (UK) rapid quench flow apparatus set in an anaerobic glovebox (Belle Technologies, Weymouth, UK) was used. Samples were quenched with 1% CF_3CO_2H and analyzed using LC−MS. Chromatographic separation was performed at 50 °C using a Waters ACQUITY BEH Amide 1.7 μm 2.1 × 100 mm column on a Waters ACQUITY ultraperformance liquid chromatography (UPLC) system (Waters Corp., Milford, MA, USA). The following eluents were used: mobile phase A: 10% H_2O, 90% acetonitrile (v/v), 10 mM ammonium formate; mobile phase B: 50% H_2O, 50% acetonitrile (v/v), 10 mM ammonium formate. The elution gradient was 0−7.0 min linear from 10% to 30% B, and 7.0−9.0 min at 10% B for re-equilibration of the column. A constant flow rate of 0.4 mL/min was used. Analytes were detected in negative ionization mode using single reaction monitoring (SRM) on a Quattro triple quadruple mass spectrometer (Waters, USA) with a cone voltage of 15 V and a capillary voltage of 3.0 kV. The desolvation temperature was set to 250 °C and the source temperature was set to 120 °C.

RESULTS

Nondenaturing ESI-MS Analyses Suggest Formation of a DAOCS·Fe(II)·2OG·penicillin N Complex. To investigate whether DAOCS can form a ternary complex with its (co)substrates, we initially carried out nondenaturing electrospray ionization-mass spectrometry (ESI-MS) studies with recombinant DAOCS.[34] Upon addition of 2 equiv of Fe(II) to DAOCS, a mass shift consistent with formation of a DAOCS·Fe(II) complex was observed by ESI-MS (Figure 2a). Increasing the Fe(II) concentration led to the observation of multiple metal binding, likely in a relatively nonspecific manner (Figure S1, Supporting Information). Attempts to substitute Fe(II) with catalytically inactive Zn(II) and Mn(II) indicated binding of multiple metal ions in the presence of excess metal ions, with the strongest binding being observed in the case of Zn(II) (Figure S1).

Addition of 2OG to the DAOCS·Fe(II) complex resulted in formation of an additional peak, with a mass corresponding to a DAOCS·Fe(II)·2OG complex (Figure 2a). Even at a 5-fold excess of 2OG relative to DAOCS, only 1 equiv of 2OG was observed to bind. Notably, in experiments with succinate substituting for 2OG, we did not observe any evidence for succinate binding (data not shown), either in the presence or

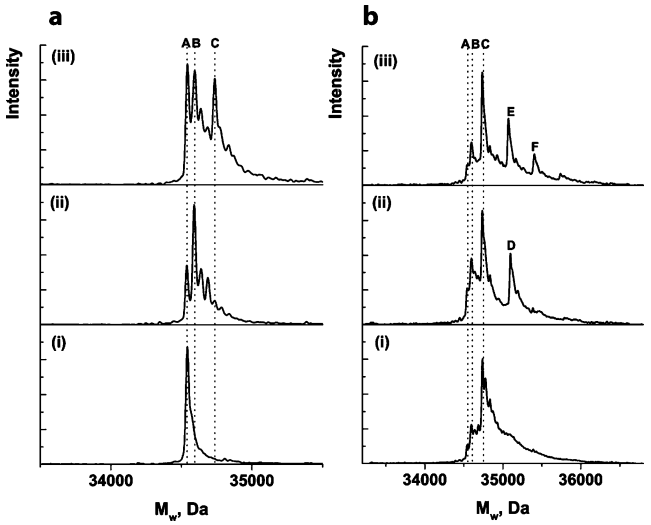

Figure 2. Nondenaturing ESI-MS analyses showing evidence for formation of ternary DAOCS·Fe(II)·NOG·penG/penN complexes. Deconvoluted spectra of cofactor and (co)substrate binding for DAOCS. (a) Conditions: (i) 15 μM DAOCS in 15 mM ammonium acetate buffer pH 7.5, (ii) 15 μM DAOCS, 30 μM Fe(II), (iii) 15 μM DAOCS, 30 μM Fe(II), 75 μM 2OG. Cone voltage: 60 V. (A – DAOCS (34545 Da), B – DAOCS·Fe(II) (34601 Da), C – DAOCS·Fe(II)·2OG (34745 Da)). (b) Conditions: (i) 15 μM DAOCS, 30 μM Fe(II), 15 μM NOG, (ii) 15 μM DAOCS, 30 μM Fe(II), 15 μM NOG, 30 μM penN, (iii) 15 μM DAOCS, 30 μM Fe(II), 15 μM NOG, 30 μM penG. Cone voltage: 60 V. (A – DAOCS (34545 Da), B – DAOCS·Fe(II) (34601 Da), C – DAOCS·Fe(II)·NOG (34747 Da). D – DAOCS·Fe(II)·NOG·penN (35107 Da), E – DAOCS·Fe·NOG·penG (35080 Da), F – DAOCS·Fe·NOG·2penG (35414 Da)). Nonspecific binding of more than 1 molecule of penG is apparent.

absence of penG (the analogue of the natural substrate, penN, used in the previous studies on DAOCS, which led to the proposal of the "ping-pong" mechanism[32]).

Since investigation of penicillin substrate binding to DAOCS·Fe(II)·2OG complex would be complicated by turnover, we replaced 2OG with the nonreactive isostere *N*-oxalylglycine (NOG). NOG showed stronger binding to the DAOCS·Fe(II) complex compared to 2OG with only 1 equiv being required for the observation of a stable complex formation (compared to 5 equiv of 2OG) (Figure 2b). We then examined binding of penN or penG to the DAOCS·Fe(II)·NOG complex. At a 2-fold excess of penG or penN (relative to DAOCS), we observed formation of a peak corresponding to the mass of a quaternary DAOCS·Fe(II)·NOG·penicillin G/N complex (Figure 2b). At higher penG or penN concentrations, additional peaks corresponding to multiple molecules of penG, but not penN, binding were observed; these additional peaks may represent noncatalytically productive binding (Figure S1). These ternary DAOCS·Fe(II)·(co)substrate complexes are analogous to those observed in equivalent experiments for other 2OG oxygenases that act via the consensus mechanism.[35,40]

NMR Water Relaxation Studies. Although the ESI-MS analyses support DAOCS catalysis proceeding via the consensus mechanism, they do not rule out the "ping-pong" mechanism. Further, the ESI-MS analyses do not necessarily reflect catalytically productive binding in solution. We thus carried out binding experiments in solution using NMR analyses of paramagnetic water relaxation.[36,37] Water molecules bound to a paramagnetic metal in the active site of metalloenzymes, including 2OG oxygenases, can be used as reporter ligands in competition experiments, thereby addressing questions on the order of substrate binding.[37]

For the purpose of experiments on DAOCS, Mn(II) was chosen as an inactive paramagnetic Fe(II) substitute that does not support catalytic turnover. ESI-MS studies indicate that Mn(II) binds to DAOCS in a similar way to Fe(II) (Figure S1); the K_d for Mn(II) binding to DAOCS was determined, followed by determination of (co)substrate binding (Table 1).

Table 1. K_d Values Determined for DAOCS Cofactor and (Co-)substrates Using the NMR Water Relaxation Method[a]

initial complex	ligand	K_d, μM
DAOCS	Mn(II)	16 ± 4
DAOCS·Mn(II)	2OG	29 ± 8
DAOCS·Mn(II)	NOG	6 ± 3
DAOCS·Mn(II)	penG	ND
DAOCS·Mn(II)·2OG	penG	ND
DAOCS·Mn(II)·2OG	penN	24 ± 6

[a]Binding curves showing changes in water relaxation times are presented in Figure S2. ND - not determined (binding was not observed within the limits of detection). PenG - penicillin G, penN - penicillin N.

Consistent with the nondenaturing ESI-MS experiments, NOG has a higher affinity for the DAOCS·Mn(II) complex (K_d(NOG) = 6 ± 3 μM) than 2OG (K_d(2OG) = 29 ± 8 μM (Table 1)). Notably, binding of penG to the DAOCS·Mn(II)·2OG complex was weak (precluding K_d determination), consistent with the previous work,[32] while penN exhibited much stronger binding. We did not observe any binding within the limit of detection of either penN or penG to the DAOCS·Mn(II) complex.

NMR Ligand Displacement Studies. According to the proposed "ping-pong" mechanism of DAOCS-catalysis, displacement of 2OG/succinate by penicillins enables binding of the latter.[29,32] To investigate possible displacement with 2OG and penG, NMR studies of 1,2,3,4-[^{13}C]-labeled 2OG (or [^{13}C]-labeled NOG) and methylene-[^{13}C]-labeled penG displacement from an inactive DAOCS·Zn(II)·2OG/penG complex were performed using 1D HSQC NMR.[39] Upon addition to the DAOCS·Zn(II) complex, the ^{13}C signal of [^{13}C]-2OG was observed to disappear (Figure 3) but to reappear upon addition of a bicyclic isoquinolinyl inhibitor (2-(1-chloro-4-hydroxyisoquinoline-3-carboxamido) acetic acid, IOX3), a known 2OG competitor for various 2OG oxygenases.[41−43] These observations suggest binding of 2OG to the DAOCS·Zn(II) complex with subsequent displacement by IOX3. When samples containing the DAOCS·Zn(II)·[^{13}C]-2OG complex were mixed with a saturating penG (50 mM) or penN (10 mM), no [^{13}C]-2OG displacement was observed (Figure 3a). The same result was obtained when [^{13}C]-labeled NOG displacement by penG from DAOCS·Fe(II)·[^{13}C]-NOG was studied (Figure S3, Supporting Information). These results further support the viability of a ternary complex intermediate during DAOCS catalysis.

Upon addition of equimolar [^{13}C]-labeled penG to the DAOCS·Zn(II) complex, complete disappearance of the [^{13}C]-penG signal was not observed, which suggests relatively weak penG binding in the absence of 2OG. Upon addition of the IOX3 inhibitor, no change in [^{13}C]-penG NMR spectrum was observed (within limits of detection), implying that binding of

dx.doi.org/10.1021/bi500086p | *Biochemistry* 2014, 53, 2483−2493

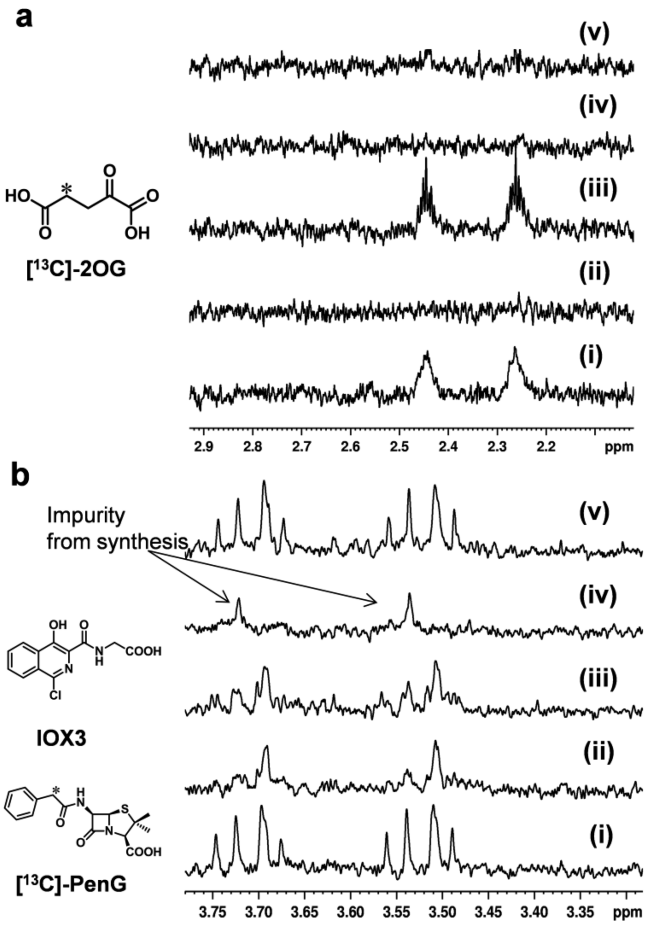

Figure 3. 1D HSQC-NMR experiments showing penG or 2OG binding to the DAOCS·Zn(II) complex. (a) Displacement experiments carried out by 1D HSQC (^{13}C selective at δ^{13}C = 30.5 ppm) using [^{13}C]-labeled 2OG. (i) [^{13}C]-2OG only; (ii) addition of [^{13}C]-2OG to DAOCS·Zn(II); (iii) addition of IOX3 to DAOCS·Zn(II)·[^{13}C]-2OG; (iv) addition of penG to DAOCS·Zn(II)·[^{13}C]-2OG; (v) addition of penN to DAOCS·Zn(II)·[^{13}C]-2OG. (b) Displacement experiments carried out by 1D HSQC (^{13}C selective at δ^{13}C = 41.8 ppm) using [^{13}C]-labeled penG. (i) [^{13}C]-penG only; (ii) addition of [^{13}C]-penG to DAOCS·Zn(II); (iii) addition of IOX3 to DAOCS·Zn(II)·[^{13}C]-penG; (iv) addition of 2OG to DAOCS·Zn(II)·[^{13}C]-penG; (v) addition of penN to DAOCS·Zn(II)·[^{13}C]-penG.

this 2OG analogue inhibitor does not interfere with (weak) penG binding. The observed weak binding of penG in the absence of 2OG is consistent with ESI-MS and Mn(II) water relaxation results (i.e., penG is likely not bound in a catalytically productive state prior to 2OG binding). If 2OG is added to the mixture instead of the inhibitor, the [^{13}C]-penG signal disappears, indicating more efficient binding of [^{13}C]-penG (Figure 3b) to the DAOCS·Zn(II)·2OG complex. Addition of excess of penN to the DAOCS, Zn(II), [^{13}C]-penG mixture, led to the reappearance of [^{13}C]-penG signal likely due to efficient displacement of [^{13}C]-penG by penN, consistent with substantially tighter binding of penN than penG.

UV−vis Studies of Ternary Complex Formation. We next employed UV−vis spectroscopy to study ternary complex formation.[7,14,44] Under anaerobic conditions, 2OG oxygenases usually show metal−ligand charge transfer (MLCT) features, centered in the 500 nm region, which represent the interaction of Fe(II) with 2OG in enzyme·Fe(II)·2OG complexes.[14,44,45] Formation of broad absorbance features was indeed apparent after addition of Fe(II) to an anaerobic solution containing DAOCS and 2OG (λ_{max} = 523nm). Saturation of Fe(II) binding (Figure 4a, inset) was achieved at 0.73 Fe(II)/DAOCS complex ratio, similar to reported values for TauD (taurine dioxygenase) and halogenase CytC3.[14,46] The determined K_d(Fe(II)) was 5.0 ± 3.7 μM. Addition of 2OG to DAOCS in the absence of Fe(II) did not result in the appearance of MLCT features.

It is proposed that binding of a "prime" substrate to the 2OG oxygenase active site promotes release of an iron-bound water molecule with a concomitant change of Fe(II) binding from a 6-coordinated to 5-coordinated state, thus promoting oxygen binding.[13,14,44] Changes in the Fe(II) coordination state can induce a shift of the UV−vis MLCT maximum (typically reducing λ_{max} by ∼10 nm, for example, from 530 to 520 nm for TauD).[44,47,48] We therefore studied the influence of substrate binding on the λ_{max} of the anaerobic DAOCS·Fe(II)·2OG complex. Upon penG addition, a shift of the maximum from λ_{max} = 523 to 519 nm was observed. Binding of penN, however, shifted the maximum further to 514 nm. Overall the UV−vis spectroscopy studies support the proposal that both penN and penG can bind to the DAOCS·Fe(II)·2OG complex, but penG binds much more weakly.

NMR Studies of the Coupling Ratio between Succinate and Penicillin Turnover. To study the 2OG coupling ratio of the DAOCS-catalyzed penN and penG reactions, steady-state ^{1}H NMR (500 MHz) analyses were performed (Figure 5a,b and Figure S4, Supporting Information). Complete (1:1) coupling of 2OG and penN oxidation was observed (within limits of detection), which did not depend on the penN and 2OG ratios. In contrast, with penG ∼20% lower coupling was observed than with penN under the same assay conditions (Figure 5c, Figure S4). In a prior report, when the 2OG concentration was increased, a decrease in penG ring expansion was observed, which was attributed to cosubstrate inhibition.[32] In our results, an increase in the 2OG/penG ratio shifts the reaction toward increased uncoupled turnover, thereby reducing levels of the penG ring expansion. We did not observe penG substrate inhibition at concentrations below 4 mM, and an increase in penG concentration led to higher 2OG and penG coupling (Figure 5).

Pre-Steady-State Kinetic Studies on the DAOCS-Catalyzed Reaction. Previous studies on pre-steady-state kinetics of TauD, vCPH (viral collagen 4-prolyl hydroxylase), the halogenase CytC3, and other 2OG oxygenases[14,46−52] have revealed that upon mixing an enzyme·Fe(II)·2OG·substrate complex with oxygen, rapid formation of a transient absorbance species with maximum at 318 nm is observed. This species is attributed to a high spin Fe(IV)-oxo intermediate by Mössbauer and Raman spectroscopy (reviewed in ref 15). In all cases the formation of this intermediate was much faster in the presence of the "prime" substrate.

In the proposed "ping-pong" mechanism for DAOCS catalysis, formation of an unusually stable Fe(IV)-oxo intermediate occurs. If this is the case, one may anticipate being able to observe such an intermediate, and its rate of formation and the reaction would be independent of the presence of penicillin. To investigate the kinetics of the formation of the proposed Fe(IV)-oxo intermediate in the DAOCS-catalyzed ring expansion reaction, stopped-flow UV−vis spectroscopy studies were carried out. Anaerobically prepared mixtures of DAOCS, Fe(II), 2OG ± penN, or

dx.doi.org/10.1021/bi500086p | Biochemistry 2014, 53, 2483−2493

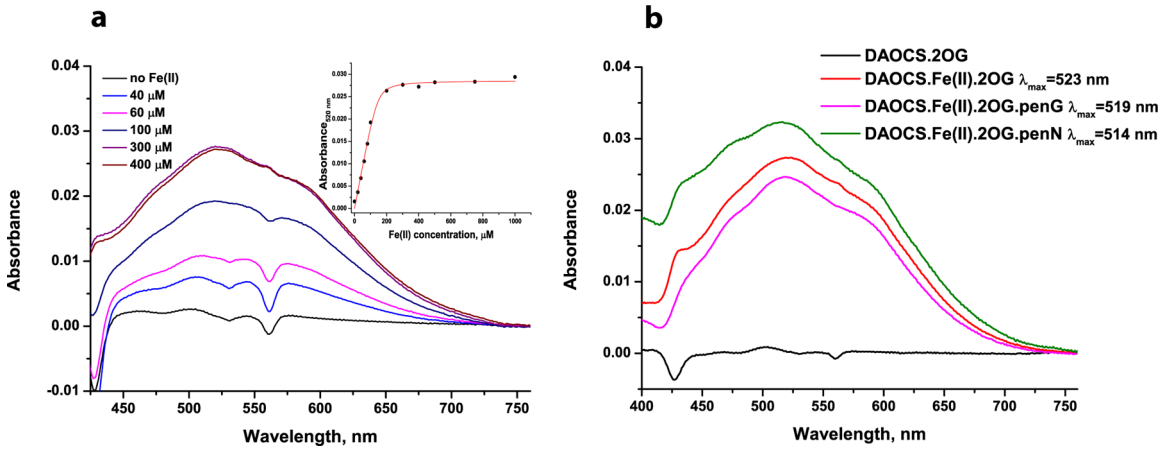

Figure 4. UV−vis spectroscopy spectra showing formation of DAOCS·Fe(II)·2OG and DAOCS·Fe(II)·2OG·penicillin G/N complexes. (a) Formation of MLCT features was observed with maxima at ∼520 nm. Conditions: 200 μM DAOCS in Hepes 50 mM (pH 7.5) was mixed with 1 mM 2OG under anaerobic conditions and titrated with Fe(II). The inset shows absorbance at 520 nm plotted as a function of Fe(II) concentration, and analysis of the dependence allowed determination of K_d(Fe(II)) = 5.0 ± 3.7 μM. (b) A shift of MLCT features maxima was observed upon addition of penicillin substrates indicating change in Fe(II) coordination. Conditions: 200 μM DAOCS in Hepes 50 mM (pH 7.5) was mixed with 1 mM 2OG, 200 μM Fe(II), and 2 mM penG/penN under anaerobic conditions.

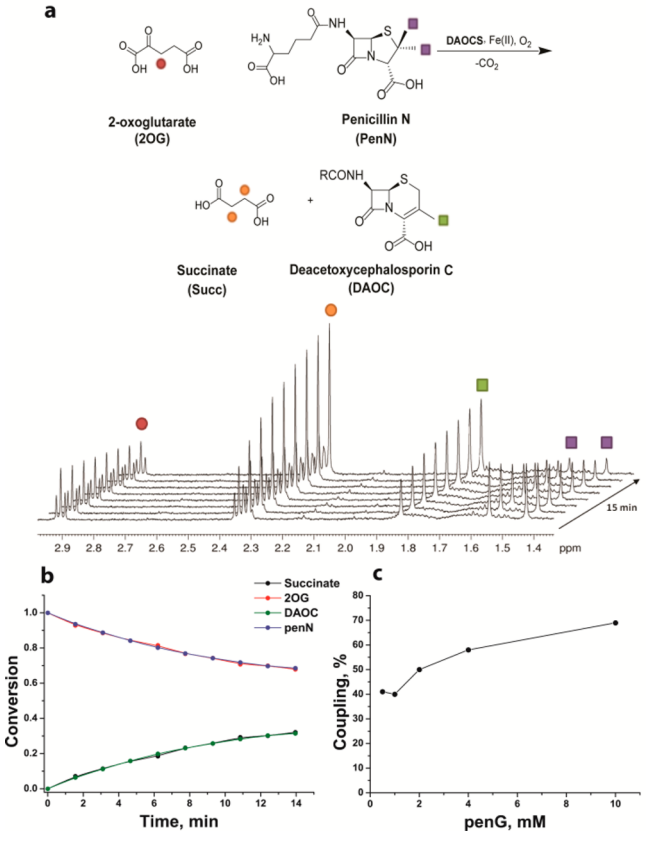

Figure 5. Steady-state ^{1}H NMR analyses of the coupling ratio between 2OG and penicillin substrate turnover. (a) ^{1}H NMR (500 MHz) spectra showing 2OG turnover is coupled to penN ring expansion. The stack spectra were acquired every 93 s. (b) Time course of 2OG and penN conversion. Conditions: 5 μM DAOCS, 50 μM Fe(II), 500 μM 2OG, 800 μM penN, 100 μM L-ascorbate. (c) Coupling between penG and 2OG conversion. Conditions: 5 μM DAOCS, 50 μM Fe(II), 500 μM 2OG, penG (varied), 100 μM L-ascorbate.

penG were rapidly mixed with oxygen-saturated buffer, and the reactions were analyzed using a photodiode array detector. Rapid formation of a transient species with maximum absorbance at 310 nm (Figure 6a), similar to those species previously reported and assigned to a high spin Fe(IV)-oxo species,[14,15,17,46,49,50,52] was observed with a maximum time of accumulation of 2 s (penN), 10 s (penG), and 25 s (uncoupled turnover) (Figure 6a and Figure S5, supporting Information). Control experiments without DAOCS showed that the observed absorbance changes do not represent formation of species derived from Fe(III) in solution (Figure S6, Supporting Information).

The kinetic traces for penN were fitted with a 2-exponential function yielding apparent rate constants (fitting parameters) for the putative intermediate formation and degradation of 1.7 s^{-1} and 0.24 s^{-1}. It was not possible to obtain good fits for the penG or uncoupled turnover reactions, which suggests a degree of heterogeneity with these systems. In the case of penG, the profile of the 310 nm species appears to consist of (at least) two highly overlapping peaks complicating further analysis (Figure 6a). This may reflect reactions including both penG ring expansion and uncoupled turnover.

After reaction of an enzyme−substrate complex with O_2, a decrease in absorbance at a wavelength corresponding to the maximum of the MLCT features (∼520 nm), representing initial enzyme·Fe(II)·2OG·substrate complex, was also observed (Figure 6b). By analogy with previous reports on other 2OG oxygenases, this intermediate may be attributed to a high-spin Fe(II) enzyme−product(s) complex, which absorbs less strongly than the initial enzyme·Fe(II)·2OG·substrate complex at 520 nm; therefore, its accumulation leads to an overall decrease in absorbance.[14,46,48] The determined rate constants of formation and degradation of this 520 nm species suggested that it is formed concurrent with degradation of the 310 nm intermediate (0.24 s^{-1} and 0.26 s^{-1} for degradation of 310 nm and formation of 520 nm species, respectively), similar to previous reports (Figure 6c).[14,46] There was only a very small decrease in the 520 nm absorbance in the absence of a "prime" substrate, consistent with the reported slow rate of uncoupled turnover.[15]

To investigate the kinetics of product formation compared to the rates of intermediate formation/decay with penN, rapid quench flow experiments were then carried out. Reactions were

dx.doi.org/10.1021/bi500086p | Biochemistry 2014, 53, 2483−2493

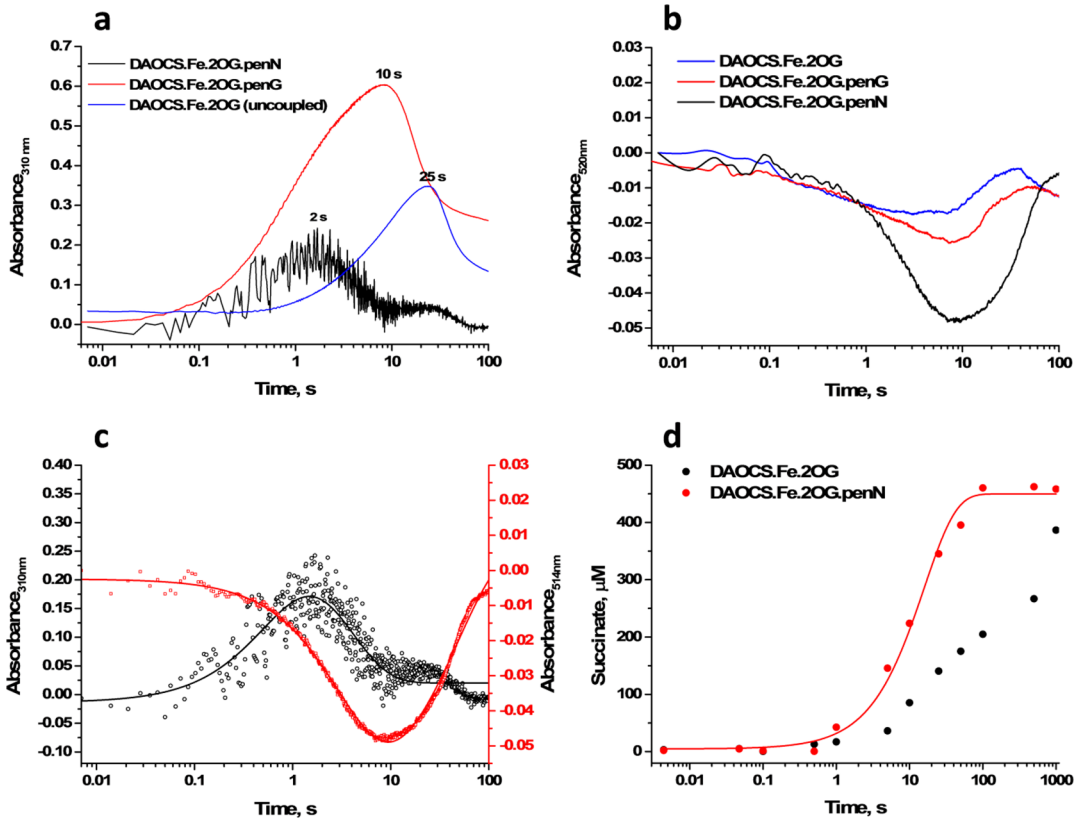

Figure 6. Transient kinetic studies showed faster formation of the putative Fe(IV)-oxo intermediate and succinate in the presence of penN compared to uncoupled turnover. Conditions: an anaerobically prepared mixture of 0.8 mM DAOCS in Hepes 50 mM (pH 7.5), 0.7 mM Fe(II), 5 mM 2OG, and 1 mM penG/penN (if present) was rapidly mixed with O_2-free/O_2-saturated buffer. Difference spectra were analyzed, and kinetic traces at (a) 310 nm and (b) 520 nm are presented. (c) 310 nm species vs 514 nm intermediate formation for DAOCS-catalyzed penN ring expansion. The data were fitted with a double exponential function. (d) Succinate accumulation detected in rapid quench flow experiments (equivalent conditions to the stopped-flow experiments) by LC−MS. Succinate concentration was determined by comparison with an external calibration curve.

performed as for the stopped-flow experiments and quenched at defined time points with 1% CF_3CO_2H. Because of the instability of penN and DAOC under acidic conditions, succinate formation was analyzed by LC−MS (steady-state NMR analyses indicated complete coupling of succinate and DAOC formation, Figure 5). In the presence of penN, succinate formation was observed with a rate constant of 0.063 s^{-1}, which is kinetically consistent with the intermediates observed spectroscopically. Succinate formation in the uncoupled reaction was estimated to occur with a rate constant of <0.01 s^{-1} and was incomplete after 1000 s. These data and the stopped-flow UV−vis spectroscopy data are consistent with penN (but not penG) triggering efficient catalysis by DAOCS.

DISCUSSION

The combined analyses reveal the viability of the formation of an enzyme·Fe(II)·2OG.penN intermediate in DAOCS catalysis. We did not accrue any evidence for the proposed "ping-pong" mechanism, in which succinate is released prior to productive penG binding (see below).[32] The results of the ESI-MS and NMR binding studies demonstrate that 2OG and penG/penN can bind simultaneously to DAOCS. Moreover, the differences in paramagnetic water relaxation times and UV−vis spectra obtained upon addition of penN to the DAOCS·Fe(II)·2OG complex demonstrate that penN binding occurs at the metal binding region of the active site without 2OG displacement. Thus, the results imply that the order of (co)substrate binding in DAOCS catalysis, at least for the natural substrate penN, likely follows the same sequence as for other studied 2OG oxygenases.[1,7,53]

There were differences, however, in observations on the binding of penN and penG. The ESI-MS and NMR studies demonstrate that penG binds much more weakly than penN, consistent with the higher K_m value for penG compared to penN (14−36 μM and 0.7−2.6 mM for penN and penG respectively).[54−57] The ESI-MS studies also suggest that penG binds in noncatalytically productive orientations as well as productive one(s). Thus, the penG crystal structures[32] (Figure S10, Supporting Information) may not represent productive complexes. Moreover, penN oxidation was fully coupled to that of 2OG within limits of detection. In contrast, for penG, a high degree of 2OG uncoupled turnover was observed. Stimulation of uncoupled 2OG turnover by noncatalytically optimal substrate binding is well-precedented with 2OG oxygenases.[1,53] The observation of increased uncoupled 2OG turnover by penG further supports the proposal that penG can bind in noncatalytically productive orientations.

Pre-steady-state kinetic studies with DAOCS reveal formation of an absorbance species at 310 nm, in the same range as for other 2OG oxygenases.[14,46,47,50] The development of a negative absorbance feature at 514−520 nm after the 310 nm absorbance species was also observed, as for other 2OG oxygenases.[7,14,46] According to the studies on other 2OG oxygenases, the Fe(IV)-oxo intermediate (318 nm species for

dx.doi.org/10.1021/bi500086p | Biochemistry 2014, 53, 2483−2493

TauD)[14] absorbs in the visible region, while a second Fe(II) intermediate (520 nm species, assigned as a high spin Fe(II)-product(s) complex) lacks the absorbance properties of the initial enzyme−substrate complex; thus the observed decay in absorbance at 520 nm occurs after degradation of the Fe(IV)-oxo intermediate (~318 nm).[7] The close analogy of the observed catalytic events for DAOCS with data for other 2OG oxygenases suggests the 310 nm species is due to an Fe(IV)-oxo intermediate; notably, formation of this species was faster in the presence of penN than with penG, or in the absence of penicillin. These observations support the consensus order of (co)substrate binding for DAOCS, rather than the "ping-pong" mechanism, in which formation of the Fe(IV)-oxo species is independent of penicillin binding.[32] Rapid quench flow analyses of the coupled and uncoupled reactions suggest that the rate of succinate formation is enhanced (at least 6-fold) by penN, implying succinate release does not occur prior to penicillin binding. Again, the results are supportive of the consensus mechanism in which binding to the enzyme·Fe(II)·2OG complex weakens chelation of an Fe(II)-coordinated water to enable O_2 binding.[7,15] The succinate formation rates support the proposal that the transiently observed species are within the catalytic pathway.

The presence of an apparent Fe(IV)-oxo intermediate species for DAOCS is consistent with the proposed radical mechanism for penicillin ring expansion, involving hydrogen abstraction from a penicillin methyl group (Figure S7, Supporting Information)[18−20] and with deuterium isotope studies using DAOC/DACS.[18,22,58] An isotope effect was observed with penN labeled on its (*pro-S*) β-methyl. Competition experiments, in which the deuterated and protiated substrates were simultaneously present,[18,58] reveal that the protiated penN is selectively transformed; such an effect was not observed in the analogous experiments with C-2 deuterated penN.[18,22,58] It was proposed that these observations reflect C-2 C-H bond cleavage after reaction of the Fe(IV)-oxo species with the (*pro-S*) β-methyl group. Evidence for this also comes from the observation that C-2 deuteration promotes formation of a C-3 hydroxycepham, a "shunt" product, that arises from hydroxylation rather than desaturation of the cepham radical intermediate (Figure S7).[22,58] These experiments were further interpreted as supporting a mechanism in which the penN can bind reversibly to an enzyme Fe(IV)-oxo species, that is, consistent with the "ping-pong" mechanism.[32] However, our mechanistic studies argue strongly for the consensus order of (co)substrate binding. We therefore propose that the selectivity of protiated versus deuterated (*pro-S*) β-methyl penN arises because the deuterated substrate is preferentially released at the stage of the Fe(IV)-oxo penicillin intermediate due to the relative difficulty in cleaving the C-^{2}H bond compared to C-^{1}H (Figure S7). This proposal implies that 2OG oxidation will be partially uncoupled for the deuterated (*pro-S*) β-methyl penN oxidation, in contrast to the reaction with DAOCS and protiated penN, where 2OG and penN oxidation is fully coupled (Figure 5).

Our results are consistent with all previously reported kinetic/solution studies, including those interpreted as being supportive of a "ping-pong" mechanism.[29,32,34,54,58,59] They are not, however, supportive of the "ping-pong" mechanism arising from crystallographic studies.[32] Structures are reported for DAOCS complexed with 2OG (PDB: 1E5I, 1RXG), succinate (PDB: 1E5H), and 2OG analogues (PDB: 1HJF, 1HJG, 2JB8), all in the H3 space group.[29,54] Structures of DAOCS complexed with penG (PDB: 1UOB) and ampicillin (PDB: 1UNB) are also reported in the same form (Figure S10, Supporting Information).[32] Subsequent structures with N-terminally His_6-tagged DAOCS were obtained, in the $P3_121$ space group, complexed with ferrous iron, ampicillin (PDB: 1W2N) and the cephalosporin product (deacetoxycephalosporin C, PDB: 1W2O).[59] The combined structures reveal a nearly identical overall fold for the DAOCS monomer including a distorted double-stranded β-helix (DSBH) fold, as in other 2OG oxygenases (Figure S8, Supporting Information).[3,4] A characteristic feature of the DAOCS subfamily is a C-terminal helix, often followed by disordered residues, which are involved in catalysis and substrate selectivity.[4,54,60,61] Evidence for the role of the C-terminus comes from studies on DAOCS, DAOCS/DACS, as well as on human enzymes, for example, the transcription factor prolyl hydroxylase isoform 2 (PHD2).[2,4,62,63] Analysis of enzyme−substrate structures for DAOCS and related 2OG oxygenases suggests they are not all, at least completely, representative of catalytically productive states. One reason is that the oligomerization required for crystallization can result in interactions that alter substrate binding (Figure S9, Supporting Information). For example, with PHD2, in one crystal form we were able to obtain only partial substrate binding due to blocking of the active site region by a loop from a crystallographically adjacent monomer.[62] In the H3 crystalline form,[32] DAOCS forms a homotrimer in which the C-terminal residues (308−311) of a monomer protrude into its active site, sterically blocking the active site and hindering penicillin binding (Figure S9). It is possible that these interactions alter the DAOCS active site such that the binding mode in the penG DAOCS complexes is not catalytically representative. Future crystallographic studies on DAOCS−substrate complexes could focus on obtaining structures not in the H3 form.

Overall, our results suggest that DAOCS employs a mechanism similar to other 2OG oxygenases, where binding of 2OG occurs first with subsequent formation of a ternary DAOCS·Fe(II)·2OG·penicillin substrate complex. The precise mechanism of the oxidative ring expansion of penN remains to be defined, but the overall evidence suggests that it most likely proceeds via a radical mediated rearrangement. Employment of unnatural substrates, for example, penG, likely can result in nonproductive substrate binding and increased uncoupled turnover. These results may be of practical significance since the effects may be used to identify DAOCS variants that more efficiently catalyze the ring expansion of hydrophobic penicillins, such as penG, yielding cephalosporins that can be more efficiently extracted than the natural cephalosporins, which have the polar D-δ-(α-aminoadipoyl) side chain.[22,54−57,61,64−67] Optimizing the ratio of 2OG and penicillin oxidation is an important parameter both with respect to improving catalytic efficiency and with respect to minimization of oxidative damage due to uncoupled turnover.[68]

■ ASSOCIATED CONTENT

Supporting Information

This study contains additional methods and Figures S1−S10. This material is available free of charge via the Internet at http://pubs.acs.org.

AUTHOR INFORMATION

Corresponding Authors

*E-mail: emily.flashman@chem.ox.ac.uk. Telephone: +44 (0) 1865 275920. Fax: +44 (0)1865 285002.
*E-mail: christopher.schofield@chem.ox.ac.uk.

Present Addresses

†(L.H.) Institute of Chemical Sciences and Engineering (ISIC), Ecole Polytechnique Fédérale de Lausanne (EPFL), 1015 Lausanne, Switzerland.
‡(A.I.) Structural Genomics Consortium, MaRS Building, 101 College Street, Toronto, M5G 1N6, Canada.

Author Contributions

#These authors contributed equally.

Funding

We thank the Wellcome Trust, European Research Council, Biotechnology & Biological Sciences Research Council (BBSRC), Clarendon - St Hugh's College - W. Louey Scholarship (H.T.), the Open Horizons program of the Dinu Patriciu Foundation (A.S.), British Heart Foundation (I.K.H.L.), Berrow Foundation (L.H.), a Royal Society Dorothy Hodgkin Fellowship and the L'Oréal-UNESCO For Women in Science Fellowship (E.F.) for financial support.

Notes

The authors declare no competing financial interest.

ACKNOWLEDGMENTS

We are grateful to Dr. E. C. Y. Woon and Dr. M. Demetriades for technical assistance and initial nondenaturing ESI-MS studies.

ABBREVIATIONS

DAOCS, deacetoxycephalosporin C synthase; DAOC, deacetoxycephalosporin C; 2OG, 2-oxoglutarate; DAOC/DACS, deacetoxycephalosporin/deacetylcephalosporin C synthase; ESI-MS, electrospray ionisation−mass spectrometry; LC−MS, liquid chromatography−mass spectrometry; NMR, nuclear magnetic resonance; penG, penicillin G; penN, penicillin N; NOG, *N*-oxalylglycine; IOX3, 2-(1-chloro-4-hydroxyisoquinoline-3-carboxamido) acetic acid; MLCT, metal ligand charge transfer; TauD, taurine dioxygenase; vCPH, viral collagen 4-prolyl hydroxylases; Hepes, 2-[4-(2-hydroxyethyl)piperazin-1-yl]ethanesulfonic acid; EDTA, ethylenediaminetetraacetic acid; SDS-PAGE, sodium dodecyl sulfate-polyacrylamide gel electrophoresis; DSBH, double-stranded β-helix; PHD2, prolyl hydroxylase domain 2

REFERENCES

(1) Hausinger, R. P. (2004) Fe(II)/α-Ketoglutarate-Dependent Hydroxylases and Related Enzymes. *Crit. Rev. Biochem. Mol. Biol. 39*, 21−68.
(2) Loenarz, C., and Schofield, C. J. (2011) Physiological and biochemical aspects of hydroxylations and demethylations catalyzed by human 2-oxoglutarate oxygenases. *Trends Biochem. Sci. 36*, 7−18.
(3) Clifton, I. J., McDonough, M. A., Ehrismann, D., Kershaw, N. J., Granatino, N., and Schofield, C. J. (2006) Structural studies on 2-oxoglutarate oxygenases and related double-stranded β-helix fold proteins. *J. Inorg. Biochem. 100*, 644−669.
(4) Aik, W., McDonough, M. A., Thalhammer, A., Chowdhury, R., and Schofield, C. J. (2012) Role of the jelly-roll fold in substrate binding by 2-oxoglutarate oxygenases. *Curr. Opin. Struct. Biol. 22*, 691−700.
(5) McDonough, M. A., Loenarz, C., Chowdhury, R., Clifton, I. J., and Schofield, C. J. (2010) Structural studies on human 2-oxoglutarate dependent oxygenases. *Curr. Opin. Struct. Biol. 20*, 659−672.
(6) Koehntop, K., Emerson, J., and Que, L., Jr. (2005) The 2-His-1-carboxylate facial triad: a versatile platform for dioxygen activation by mononuclear non-heme iron(II) enzymes. *J. Biol. Inorg. Chem. 10*, 87−93.
(7) Bollinger, J. M., Price, J. C., Hoffart, L. M., Barr, E. W., and Krebs, C. (2005) Mechanism of taurine α-ketoglutarate dioxygenase (TauD) from *Escherichia coli*. *Eur. J. Inorg. Chem. 2005*, 4245−4254.
(8) Bollinger, J. M., Jr., and Krebs, C. (2007) Enzymatic C−H activation by metal−superoxo intermediates. *Curr. Opin. Chem. Biol. 11*, 151−158.
(9) Solomon, E. I., Brunold, T. C., Davis, M. I., Kemsley, J. N., Lee, S.-K., Lehnert, N., Neese, F., Skulan, A. J., Yang, Y.-S., and Zhou, J. (1999) Geometric and Electronic Structure/Function Correlations in Non-Heme Iron Enzymes. *Chem. Rev. 100*, 235−350.
(10) Solomon, E. I., Decker, A., and Lehnert, N. (2003) Non-heme iron enzymes: Contrasts to heme catalysis. *Proc. Natl. Acad. Sci. U. S. A. 100*, 3589−3594.
(11) Grzyska, P. K., Appelman, E. H., Hausinger, R. P., and Proshlyakov, D. A. (2010) Insight into the mechanism of an iron dioxygenase by resolution of steps following the FeIV=O species. *Proc. Natl. Acad. Sci. U. S. A. 107*, 3982−3987.
(12) Pavel, E. G., Zhou, J., Busby, R. W., Gunsior, M., Townsend, C. A., and Solomon, E. I. (1998) Circular dichroism and magnetic circular dichroism spectroscopic studies of the non-heme ferrous active site in clavaminate synthase and its interaction with α-ketoglutarate cosubstrate. *J. Am. Chem. Soc. 120*, 743−753.
(13) Light, K. M., Hangasky, J. A., Knapp, M. J., and Solomon, E. I. (2013) Spectroscopic studies of the mononuclear non-heme Fe(II) enzyme FIH: second-sphere contributions to reactivity. *J. Am. Chem. Soc. 135*, 9665−9674.
(14) Price, J. C., Barr, E. W., Tirupati, B., Bollinger, J. M., and Krebs, C. (2003) The first direct characterization of a high-valent iron intermediate in the reaction of an α-ketoglutarate-dependent dioxygenase: a high-spin Fe(IV) complex in taurine/α-ketoglutarate dioxygenase (TauD) from *Escherichia coli*. *Biochemistry 42*, 7497−7508.
(15) Krebs, C., Galonić Fujimori, D., Walsh, C. T., and Bollinger, J. M. (2007) Non-heme Fe(IV)−oxo intermediates. *Acc. Chem. Res. 40*, 484−492.
(16) Price, J. C., Barr, E. W., Glass, T. E., Krebs, C., and Bollinger, J. M. (2003) Evidence for Hydrogen Abstraction from C1 of Taurine by the High-Spin Fe(IV) Intermediate Detected during Oxygen Activation by Taurine:α-Ketoglutarate Dioxygenase (TauD). *J. Am. Chem. Soc. 125*, 13008−13009.
(17) Riggs-Gelasco, P. J., Price, J. C., Guyer, R. B., Brehm, J. H., Barr, E. W., Bollinger, J. M., and Krebs, C. (2004) EXAFS Spectroscopic Evidence for an FeO Unit in the Fe(IV) Intermediate Observed during Oxygen Activation by Taurine:α-Ketoglutarate Dioxygenase. *J. Am. Chem. Soc. 126*, 8108−8109.
(18) Baldwin, J. E., Adlington, R. M., Aplin, R. T., Crouch, N. P., Knight, G., and Schofield, C. J. (1987) Cephalosporin C biosynthesis; a branched pathway sensitive to a kinetic isotope effect. *J. Chem. Soc., Chem. Commun.*, 1651−1654.
(19) Townsend, C. A., Theis, A. B., Neese, A. S., Barrabee, E. B., and Poland, D. (1985) Stereochemical fate of chiral methyl of valine in the ring expansion of penicillin N to deacetoxycephalosporin C. *J. Am. Chem. Soc. 107*, 4760−4767.
(20) Pang, C. P., White, R. L., Abraham, E. P., Crout, D. H., Lutstorf, M., Morgan, P. J., and Derome, A. E. (1984) Stereochemistry of the incorporation of valine methyl groups into methylene groups in cephalosporin C. *Biochem. J. 222*, 777−788.
(21) Hewitson, K. S., Liénard, B. M. R., McDonough, M. A., Clifton, I. J., Butler, D., Soares, A. S., Oldham, N. J., McNeill, L. A., and Schofield, C. J. (2007) Structural and mechanistic studies on the inhibition of the hypoxia-inducible transcription factor hydroxylases by tricarboxylic acid cycle intermediates. *J. Biol. Chem. 282*, 3293−3301.

(22) Hamed, R. B., Gomez-Castellanos, J. R., Henry, L., Ducho, C., McDonough, M. A., and Schofield, C. J. (2013) The enzymes of β-lactam biosynthesis. *Nat. Prod. Rep. 30*, 21−107.
(23) Baldwin, J. E., Adlington, R. M., Coates, J. B., Crabbe, M. J., Crouch, N. P., Keeping, J. W., Knight, G. C., Schofield, C. J., Ting, H. H., and Vallejo, C. A. (1987) Purification and initial characterization of an enzyme with deacetoxycephalosporin C synthetase and hydroxylase activities. *Biochem. J. 245*, 831−841.
(24) Dotzlaf, J. E., and Yeh, W. K. (1987) Copurification and characterization of deacetoxycephalosporin C synthetase/hydroxylase from Cephalosporium acremonium. *J. Bacteriol. 169*, 1611−1618.
(25) Kovacevic, S., Weigel, B. J., Tobin, M. B., Ingolia, T. D., and Miller, J. R. (1989) Cloning, characterization, and expression in Escherichia coli of the Streptomyces clavuligerus gene encoding deacetoxycephalosporin C synthetase. *J. Bacteriol. 171*, 754−760.
(26) Baker, B. J., Dotzlaf, J. E., and Yeh, W. K. (1991) Deacetoxycephalosporin C hydroxylase of Streptomyces clavuligerus. Purification, characterization, bifunctionality, and evolutionary implication. *J. Biol. Chem. 266*, 5087−5093.
(27) Rollins, M. J., Westlake, D. W. S., Wolfe, S., and Jensen, S. E. (1988) Purification and initial characterization of deacetoxycephalosporin C synthase from Streptomyces clavuligerus. *Can. J. Microbiol. 34*, 1196−1202.
(28) Tahlan, K., and Jensen, S. E. (2013) Origins of the β-lactam rings in natural products. *J. Antibiot. 66*, 401−410.
(29) Valegard, K., van Scheltinga, A. C. T., Lloyd, M. D., Hara, T., Ramaswamy, S., Perrakis, A., Thompson, A., Lee, H.-J., Baldwin, J. E., Schofield, C. J., Hajdu, J., and Andersson, I. (1998) Structure of a cephalosporin synthase. *Nature 394*, 805−809.
(30) Burzlaff, N. I., Rutledge, P. J., Clifton, I. J., Hensgens, C. M. H., Pickford, M., Adlington, R. M., Roach, P. L., and Baldwin, J. E. (1999) The reaction cycle of isopenicillin N synthase observed by X-ray diffraction. *Nature 401*, 721−724.
(31) Freed, J. D., Hart, D. J., and Magomedov, N. A. (2001) Trapping of the putative cationic intermediate in the Morin rearrangement with carbon nucleophiles. *J. Org. Chem. 66*, 839−852.
(32) Valegard, K., van Scheltinga, A. C. T., Dubus, A., Ranghino, G., Oster, L. M., Hajdu, J., and Andersson, I. (2004) The structural basis of cephalosporin formation in a mononuclear ferrous enzyme. *Nat. Struct. Mol. Biol. 11*, 95−101.
(33) Baldwin, J. E., Adlington, R. M., Kang, T. W., Lee, E., and Schofield, C. J. (1988) The ring expansion of penama to cephams: a possible biomimetic process. *Tetrahedron 44*, 5953−5957.
(34) Lloyd, M. D., Lee, H.-J., Harlos, K., Zhang, Z.-H., Baldwin, J. E., Schofield, C. J., Charnock, J. M., Garner, C. D., Hara, T., Terwisscha van Scheltinga, A. C., Valegård, K., Viklund, J. A. C., Hajdu, J., Andersson, I., Danielsson, Å., and Bhikhabhai, R. (1999) Studies on the active site of deacetoxycephalosporin C synthase. *J. Mol. Biol. 287*, 943−960.
(35) Mecinović, J., Chowdhury, R., Flashman, E., and Schofield, C. J. (2009) Use of mass spectrometry to probe the nucleophilicity of cysteinyl residues of prolyl hydroxylase domain 2. *Anal. Biochem. 393*, 215−221.
(36) Leung, I. K. H., Flashman, E., Yeoh, K. K., Schofield, C. J., and Claridge, T. D. W. (2010) Using NMR solvent water relaxation to investigate metalloenzyme-ligand binding interactions. *J. Med. Chem. 53*, 867−875.
(37) Bertini, I., Fragai, M., Luchinat, C., and Talluri, E. (2008) Water-Based Ligand Screening for Paramagnetic Metalloproteins. *Angew. Chem., Int. Ed. 47*, 4533−4537.
(38) Morton, C. J., Pugh, D. J. R., Brown, E. L. J., Kahmann, J. D., Renzoni, D. A. C., and Campbell, I. D. (1996) Solution structure and peptide binding of the SH3 domain from human Fyn. *Structure 4*, 705−714.
(39) Leung, I. K. H., Demetriades, M., Hardy, A. P., Lejeune, C., Smart, T. J., Szöllössi, A., Kawamura, A., Schofield, C. J., and Claridge, T. D. W. (2013) Reporter ligand NMR screening method for 2-oxoglutarate oxygenase inhibitors. *J. Med. Chem. 56*, 547−555.
(40) McNeill, L. A., Flashman, E., Buck, M. R. G., Hewitson, K. S., Clifton, I. J., Jeschke, G., Claridge, T. D. W., Ehrismann, D., Oldham, N. J., and Schofield, C. J. (2005) Hypoxia-inducible factor prolyl hydroxylase 2 has a high affinity for ferrous iron and 2-oxoglutarate. *Mol. Biosyst. 1*, 321−324.
(41) McDonough, M. A., Li, V., Flashman, E., Chowdhury, R., Mohr, C., Liénard, B. M. R., Zondlo, J., Oldham, N. J., Clifton, I. J., Lewis, J., McNeill, L. A., Kurzeja, R. J. M., Hewitson, K. S., Yang, E., Jordan, S., Syed, R. S., and Schofield, C. J. (2006) Cellular oxygen sensing: Crystal structure of hypoxia-inducible factor prolyl hydroxylase (PHD2). *Proc. Natl. Acad. Sci. U. S. A. 103*, 9814−9819.
(42) Warshakoon, N. C., Wu, S., Boyer, A., Kawamoto, R., Sheville, J., Renock, S., Xu, K., Pokross, M., Evdokimov, A. G., Walter, R., and Mekel, M. (2006) A novel series of imidazo[1,2-a]pyridine derivatives as HIF-1α prolyl hydroxylase inhibitors. *Bioorg. Med. Chem. Lett. 16*, 5598−5601.
(43) Aik, W., Demetriades, M., Hamdan, M. K. K., Bagg, E. A. L., Yeoh, K. K., Lejeune, C., Zhang, Z., McDonough, M. A., and Schofield, C. J. (2013) Structural Basis for Inhibition of the Fat Mass and Obesity Associated Protein (FTO). *J. Med. Chem. 56*, 3680−3688.
(44) Ryle, M. J., Padmakumar, R., and Hausinger, R. P. (1999) Stopped-flow kinetic analysis of Escherichia coli taurine/α-ketoglutarate dioxygenase: interactions with α-ketoglutarate, taurine, and oxygen. *Biochemistry 38*, 15278−15286.
(45) Ryle, M. J., Liu, A., Muthukumaran, R. B., Ho, R. Y. N., Koehntop, K. D., McCracken, J., Que, L., and Hausinger, R. P. (2003) O_2- and α-Ketoglutarate-Dependent Tyrosyl Radical Formation in TauD, an α-Keto Acid-Dependent Non-Heme Iron Dioxygenase. *Biochemistry 42*, 1854−1862.
(46) Hoffart, L. M., Barr, E. W., Guyer, R. B., Bollinger, J. M., and Krebs, C. (2006) Direct spectroscopic detection of a C-H-cleaving high-spin Fe(IV) complex in a prolyl-4-hydroxylase. *Proc. Natl. Acad. Sci. U. S. A. 103*, 14738−14743.
(47) Sánchez-Fernández, E. M., Tarhonskaya, H., Al-Qahtani, K., Hopkinson, R. J., McCullagh, J. S. O., Schofield, C. J., and Flashman, E. (2013) Investigations on the oxygen dependence of a 2-oxoglutarate histone demethylase. *Biochem. J. 449*, 491−496.
(48) Grzyska, P. K., Ryle, M. J., Monterosso, G. R., Liu, J., Ballou, D. P., and Hausinger, R. P. (2005) Steady-State and Transient Kinetic Analyses of Taurine/α-Ketoglutarate Dioxygenase: Effects of Oxygen Concentration, Alternative Sulfonates, and Active-Site Variants on the FeIV-oxo Intermediate. *Biochemistry 44*, 3845−3855.
(49) Galonic, D. P., Barr, E. W., Walsh, C. T., Bollinger, J. M., and Krebs, C. (2007) Two interconverting Fe(IV) intermediates in aliphatic chlorination by the halogenase CytC3. *Nat. Chem. Biol. 3*, 113−116.
(50) Matthews, M. L., Krest, C. M., Barr, E. W., Vaillancourt, F. d. r. H., Walsh, C. T., Green, M. T., Krebs, C., and Bollinger, J. M. (2009) Substrate-triggered formation and remarkable stability of the C−H bond-cleaving chloroferryl Intermediate in the aliphatic halogenase, SyrB2. *Biochemistry 48*, 4331−4343.
(51) Flashman, E., Hoffart, L. M., Hamed, R. B., Bollinger, J. M., Jr, Krebs, C., and Schofield, C. J. (2010) Evidence for the slow reaction of hypoxia-inducible factor prolyl hydroxylase 2 with oxygen. *FEBS J. 277*, 4089−4099.
(52) Price, J. C., Barr, E. W., Hoffart, L. M., Krebs, C., and Bollinger, J. M. (2005) Kinetic Dissection of the Catalytic Mechanism of Taurine:α-Ketoglutarate Dioxygenase (TauD) from *Escherichia coli*. *Biochemistry 44*, 8138−8147.
(53) Hewitson, K. S., Granatino, N., Welford, R. W. D., McDonough, M. A., and Schofield, C. J. (2005) Oxidation by 2-oxoglutarate oxygenases: non-haem iron systems in catalysis and signalling. *Philos. Trans. Math. Phys. Eng. Sci. 363*, 807−828.
(54) Lee, H.-J., Lloyd, M. D., Harlos, K., Clifton, I. J., Baldwin, J. E., and Schofield, C. J. (2001) Kinetic and crystallographic studies on deacetoxycephalosporin C synthase (DAOCS). *J. Mol. Biol. 308*, 937−948.

(55) Lee, H.-J., Schofield, C. J., and Lloyd, M. D. (2002) Active site mutations of recombinant Deacetoxycephalosporin C Synthase. *Biochem. Biophys. Res. Commun. 292*, 66−70.
(56) Ji, J., Tian, X., Fan, K., and Yang, K. (2012) New strategy of site-directed mutagenesis identifies new sites to improve Streptomyces clavuligerus deacetoxycephalosporin C synthase activity toward penicillin G. *Appl. Microbiol. Biotechnol. 93*, 2395−2401.
(57) Wei, C.-L., Yang, Y.-B., Wang, W.-C., Liu, W.-C., Hsu, J.-S., and Tsai, Y.-C. (2003) Engineering streptomyces clavuligerus deacetoxycephalosporin C synthase for optimal ring expansion activity toward penicillin G. *Appl. Environ. Microbiol. 69*, 2306−2312.
(58) Baldwin, J. E., Adlington, R. M., Crouch, N. P., Schofield, C. J., Turner, N. J., and Aplin, R. T. (1991) Cephalosporin biosynthesis: A branched pathway sensitive to an isotope effect. *Tetrahedron 47*, 9881−9900.
(59) Öster, L. M., van Scheltinga, A. C. T., Valegård, K., Hose, A. M., Dubus, A., Hajdu, J., and Andersson, I. (2004) Conformational flexibility of the C terminus with implications for substrate binding and catalysis revealed in a new crystal form of deacetoxycephalosporin C synthase. *J. Mol. Biol. 343*, 157−171.
(60) Chin, H. S., and Sim, T. S. (2002) C-terminus modification of Streptomyces clavuligerus deacetoxycephalosporin C synthase improves catalysis with an expanded substrate specificity. *Biochem. Biophys. Res. Commun. 295*, 55−61.
(61) Lloyd, M. D., Lipscomb, S. J., Hewitson, K. S., Hensgens, C. M. H., Baldwin, J. E., and Schofield, C. J. (2004) Controlling the substrate selectivity of deacetoxycephalosporin/deacetylcephalosporin C synthase. *J. Biol. Chem. 279*, 15420−15426.
(62) Chowdhury, R., McDonough, M. A., Mecinović, J., Loenarz, C., Flashman, E., Hewitson, K. S., Domene, C., and Schofield, C. J. (2009) Structural basis for binding of hypoxia-inducible factor to the oxygen-sensing prolyl hydroxylases. *Structure 17*, 981−989.
(63) Flashman, E., Bagg, E. A. L., Chowdhury, R., Mecinović, J., Loenarz, C., McDonough, M. A., Hewitson, K. S., and Schofield, C. J. (2008) Kinetic rationale for selectivity toward N- and C-terminal oxygen-dependent degradation domain substrates mediated by a loop region of hypoxia-Inducible factor prolyl hydroxylases. *J. Biol. Chem. 283*, 3808−3815.
(64) Chin, H. S., Sim, J., and Sim, T. S. (2001) Mutation of N304 to leucine in Streptomyces clavuligerus deacetoxycephalosporin C synthase creates an enzyme with increased penicillin analogue conversion. *Biochem. Biophys. Res. Commun. 287*, 507−513.
(65) Goo, K. S., Chua, C. S., and Sim, T.-S. (2008) A complete library of amino acid alterations at R306 in Streptomyces clavuligerus deacetoxycephalosporin C synthase demonstrates its structural role in the ring-expansion activity. *Proteins: Struct., Funct., Bioinf. 70*, 739−747.
(66) Goo, K. S., Chua, C. S., and Sim, T.-S. (2008) Relevant double mutations in bioengineered Streptomyces clavuligerus deacetoxycephalosporin C synthase result in higher binding specificities which improve penicillin bioconversion. *Appl. Environ. Microbiol. 74*, 1167−1175.
(67) Goo, K.-S., Chua, C.-S., and Sim, T.-S. (2009) Directed evolution and rational approaches to improving Streptomyces clavuligerus deacetoxycephalosporin C synthase for cephalosporin production. *J. Ind. Microbiol. Biotechnol. 36*, 619−633.
(68) Mantri, M., Zhang, Z., McDonough, M. A., and Schofield, C. J. (2012) Autocatalysed oxidative modifications to 2-oxoglutarate dependent oxygenases. *FEBS J. 279*, 1563−1575.